Cold Regions Science and Technology, 6 (1983) 257–266
Elsevier Scientific Publishing Company, Amsterdam – Printed in The Netherlands

THE PREDICTION OF EXTREME KEEL DEPTHS FROM SEA ICE PROFILES

Peter Wadhams

Scott Polar Research Institute, University of Cambridge, Cambridge CB2 1ER (U.K.)

(Received May 10, 1982; accepted in revised form October 21, 1982)

ABSTRACT

The prediction of return periods of extremely deep pressure ridge keels is discussed, using as data a 1400 km submarine profile obtained by U.S.S. "Gurnard" in the Beaufort Sea. Three techniques of predicting return periods at a point are examined: the use of the negative exponential distribution; a depth crossing technique; and a probability plotting technique. The problem of predicting return periods along a line is then examined with reference to ice scouring across seabed pipeline routes. A technique which combines keel statistics and scour depth statistics is used to compute the pipeline burial depth necessary to avoid disturbance by ice for a specified period.

INTRODUCTION

A fundamental problem in the estimation of return periods for deep keels *at a point* is that of predicting extreme values from a time series or spatial profile of limited extent. In this paper we examine three techniques of prediction, and compare their performances using a data set in the public domain. We then examine the problem of predicting extreme keel depths *along a line*, i.e. the probability that a pipeline route will suffer scouring by a keel during a given interval. We propose two ways of attacking this problem, and consider an example of how to predict pipeline burial depths using these statistics.

THE DATA SET

The pressure ridge distribution in the Beaufort Sea coastal environment is highly variable, both in time and space. The best way of obtaining data suitable for keel depth prediction at a given location is therefore to employ a bottom-mounted upward-looking sonar at that location to record continuously for a year or more (Hoare et al., 1980). This gives a time series which is site-specific and which is free of bias due to improper estimation of mean ice drift velocity (a drawback of spatial profiles). It also avoids the problem of estimating how the local bottom topography affects the likelihood of keel scouring at that location, i.e. whether there is a sheltering effect on point A due to keels grounding at a nearby point B and distorting the local ice velocity and deformation fields so as to reduce the likelihood of a grounding at A.

Data obtained by this technique are not as yet in the public domain, so to examine various techniques of extreme draft prediction we employ a data set which has already been analysed (Wadhams and Horne, 1980, henceforth WH), a 1400 km submarine sonar profile from the southern Beaufort Sea obtained by U.S.S. "Gurnard" in April 1976. The beam width of the sonar (2°) was very small and so this record represents the best quality of all submarine sonar profiles available to date. Figure 1 shows the track of "Gurnard", beginning at the 100 m isobath off Barter Island; the track was divided into 50 km sections for WH's statistical analysis, section 1 beginning at O.

EXTREME DEPTH PREDICTIONS AT A POINT

Technique 1: Use of the negative exponential distribution

WH defined an independent keel as one in which the troughs (points of minimum draft) on either side of the keel crest (point of maximum draft) each rise

0165-232X/83/$03.00

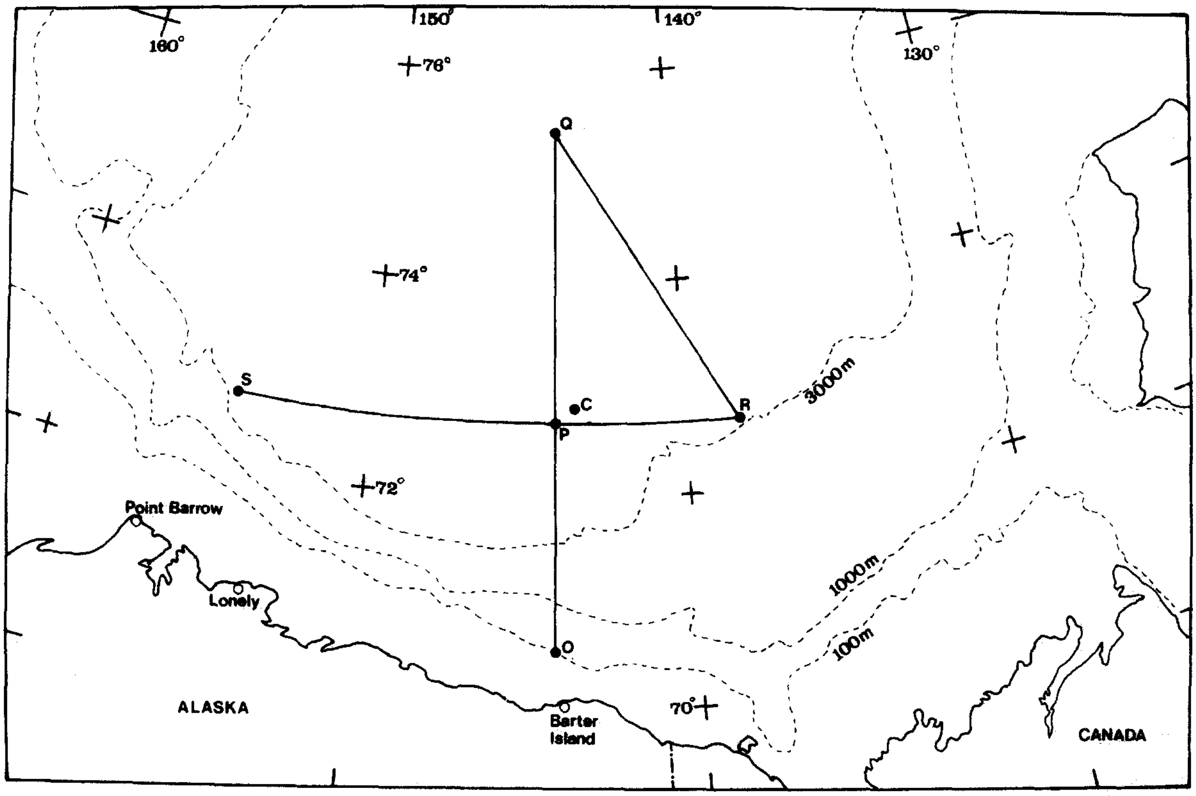

Fig. 1. Route of U.S.S. "Gurnard", 7–10 April 1976 (after Wadhams and Horne, 1980).

at least half way towards the local level ice bottom before beginning to descend again. The "local level ice bottom" is difficult to find, especially in heavily ridged areas, so it is defined arbitrarily as being a draft of 2.5 m. This is the Rayleigh criterion for ridge definition; it is one of an infinite range of possible empirical criteria, but is the most common in published analyses of sonar and laser profiles (Leppäranta, 1981; Lowry and Wadhams, 1979; Tucker et al., 1979; Wadhams, 1976, 1978, 1980, 1981; Wadhams and Lowry, 1977; Weeks et al., 1980; Williams et al., 1975).

Using this criterion WH found that the number of keels per km of track per metre of draft increment, $n(h)$, was related to the draft h by a negative exponential distribution:

$$n(h)\mathrm{d}h = B \exp(-bh)\mathrm{d}h \qquad (1)$$

where the parameters B and b can be expressed in terms of the experimentally observed mean keel draft $\bar{h}$, mean number of keels per km μ, and low value cut-off draft h_0:

$$b = (\bar{h} - h_0)^{-1} \qquad (2)$$

$$B = \mu b \exp(bh_0) \qquad (3)$$

The fit of the data to this distribution was extremely good, as shown in Fig. 2.

The negative exponential distribution has been found to fit sail heights as measured by laser profilometers (Leppäranta, 1981; Tucker et al., 1979; Wadhams, 1976, 1980, 1981; Weeks et al., 1980) as well as keel drafts. However, keel drafts measured by a wide beam sonar in the Eurasian Basin (Wadhams, 1981) were found to fit a distribution proposed by Hibler et al. (1972), of form

$$n(h) \propto \exp(-\lambda h^2) \qquad (4)$$

although with some deviation towards (1) at extreme depths. It is reasonable to conclude that this is due to

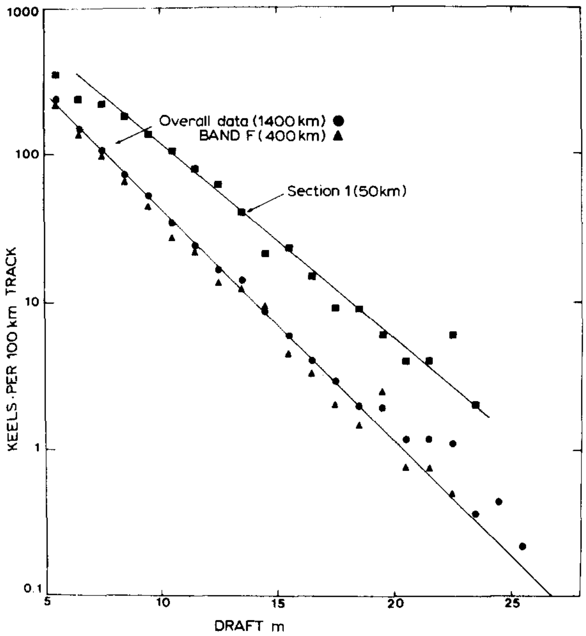

Fig. 2. Distribution of keel drafts for whole data set; section 1 only (50 km beginning at point O on Fig. 1); and a 400 km section from the central Beaufort Sea (along leg RPS on Fig. 1). Bin size 1 m (after Wadhams and Horne, 1980).

the effect of beam width upon the shape of the under-ice profile and that (1), since it fits narrow-beam data, is an equation of more general validity for ridge keels.

Using (1) we can estimate the total number of keels *per year* passing a given point and having depths of D or greater, as follows:

$$N_D = L \int_D^\infty n(h)\mathrm{d}h = L\,\mu \exp\left[-\frac{D-h_0}{\bar{h}-h_0}\right] \tag{5}$$

where L km is the distance drifted per year by the ice cover over that point. If D is the water depth, then N_D is the number of grounding ridges at that site per year, i.e. the number of scouring events. $(1/N_D)$ is the ***return period in years***, T_D, for a keel of depth D or greater.

$$T_D = 1/N_D \tag{6}$$

In order to calculate T_D from (5) we need to know L. This is a site-specific quantity, but typical values would be 500 km in the transition zone and 1000 km over deep water in the southern Beaufort Sea. The best data come from buoys (NORCOR, 1977; Thorndike and Colony, 1980b, 1981) and the AIDJEX experiment provided a year's data relevant to the central Beaufort Sea (Thorndike and Colony, 1980a; L = 2100 km). Having taken a best value for L from available data, we proceed either by taking values for $\bar{h}$ and μ from the 50 km sections, or by actually plotting out the observed data on semi-logarithmic paper as in Fig. 2 and extrapolating the line of best fit. The results from these procedures will differ slightly since, as Fig. 2 shows, there is some deviation from a negative exponential at low drafts (e.g. section 1, 5–8 m depth) and at extremely high drafts. The low draft deviation occurs because some features which are not ridges appear in the statistics, e.g. deep floe bottoms. The high draft deviation occurs mainly because of the very small numbers of keels per depth increment ("bin") counted at deep draft, making the statistics unreliable. The best procedure is therefore to plot out the data, to ignore the shallow end of the curve if it deviates from a negative exponential, to ignore the very deep end when there are, say, fewer than 10 keels per bin, and to fit the rest of the curve to a negative exponential so as to obtain b and B from the gradient and intercept. A quicker procedure is simply to use $\bar{h}$ and μ from the statistics computed for a high h_0 (say 9 m) since the higher cut-off removes the low draft deviation.

As an illustration, we use the quick procedure to compute T_D for two cases:

(1) The mean of the whole 1400 km putting L = 1000 km, assumed to be typical of the southern Beaufort Sea.

(2) The mean of sections 1 and 2, (the 100 km beginning at O) putting L = 500 km, assumed to be typical of the transition zone.

The results are shown in Table 1.

Note the very large difference – up to a factor of 10 – between the return periods deep in the Arctic Ocean and the periods in the heavily ridged coastal environment. The return period which is of interest in practice, e.g. the desired interval between scouring events at a sea bottom wellhead, is of order 1000 years. In case 2 this occurs at about 55 m water depth.

If the return period is specified, then (5) and (6) can be rearranged to give the keel depth at which the required return period occurs:

$$D = h_0 + (\bar{h} - h_0)\ln(T_D\,L\mu) \tag{7}$$

TABLE 1

Extreme depth predictions using negative exponential distribution

D (m)	T_D, case 1	T_D, case 2
25	1.6 months	27 days
30	9.2 months	4.4 months
35	4.3 years	1.76 years
40	24.3	8.50
45	136	41.1
50	767	199
55	4310	959
60	24,300	4,630
65	136,000	22,400
70	767,000	108,000
80	2.43×10^7	2.52×10^6
90	7.67×10^8	5.87×10^7
100	2.43×10^{10}	1.37×10^9

This varies more strongly with the mean keel draft $\bar{h}$ than with the number of keels passing the site per year ($L\mu$).

Technique 2: Distances between depth crossings

Technique 1 depends for its success on the fact that the keel drafts follow a particularly simple mathematical distribution, thanks to the high quality of the data. We have already mentioned wide-beam data which follow a different distribution, although tending towards the negative exponential at great depths. In future it is likely that extensive wide-beam data from early U.S. Navy cruises to the Beaufort Sea will be declassified. We need a technique to handle such data, since even when bottom detail has been smoothed out by the beamwidth it ought to be possible to manipulate the data so that extreme value predictions are similar to those from good data.

A technique which avoids the use of an arbitrary ridge-defining criterion is to look at the statistics of crossings of a given depth horizon by the ice bottom profile. In Fig. 3, let $X(h)$ be the set of distances between an upward crossing of a depth horizon h and the subsequent downward crossing of the same horizon. The probability density function of $X(h)$ will consist partly of very small values due to the intervals between peaks within a single keel, and partly of large values due to the spacings between keels. The mean value $\bar{X}(h)$, however, should increase monotonically with h except where h is so small that $X(h)$ is just the distribution of lead widths. If $\bar{X}(h)$ is a simple mathematical function of h, then we can extrapolate beyond the range of measured values to obtain $\bar{X}(h)$ at very large h. This is then the return spacing between keels of depth h or larger, and so the return period T_D is simply

$$T_D = \bar{X}(D)/L \tag{8}$$

Figure 4 shows the result of computing $\bar{X}(h)$ for the two cases of the whole data set and of sections 1 and 2 alone. The computation was carried out at 2 m intervals starting at h = 4 m. For the overall data, the range from h = 6 m to h = 22 m fits an exponential distribution, while for sections 1 and 2 the fit extends from 4 m to 22 m. From 24 m upwards there are too few values for valid statistics. The fit to an exponential distribution was a likely, but not inevitable, consequence of the keel draft distribution having a negative

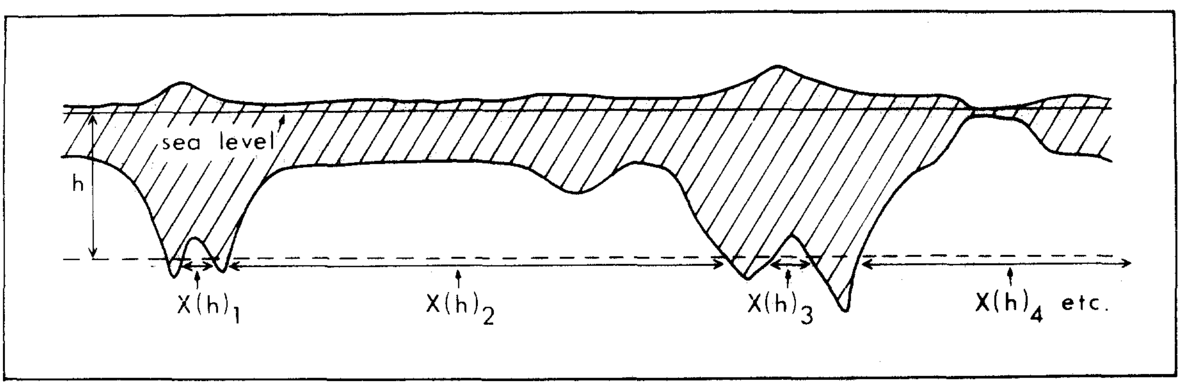

Fig. 3. The depth crossing technique.

TABLE 2

Extreme depth predictions using depth crossing technique

D (m)	T_D, case 1	T_D, case 2
25	1.3 months	22 days
30	8.1 months	3.9 months
35	4.2 years	1.78 years
,40	26.2	9.66
45	163	52.5
50	1010	286
55	6280	1550
60	39,100	8450
65	243,000	46,000
70	1.51×10^6	250,000
80	5.84×10^7	7.30×10^6
90	2.26×10^9	2.19×10^8
100	8.74×10^{10}	6.48×10^9

exponential form. By fitting regression lines to the valid parts of Figure 4 and using (8), we obtain the following predictions for T_D (Table 2).

Comparison of Table 2 with Table 1 shows good agreement. Standard deviations were estimated from the goodness of fit of the regression lines, and were found to be almost identical for each technique. For case 1 the uncertainty is ±3% at D = 25 m, increasing approximately linearly to ±24% at D = 100 m; for case 2 the figures are ±4% and ±32%. In most cases the two techniques give predictions which agree to within one standard deviation. The techniques are

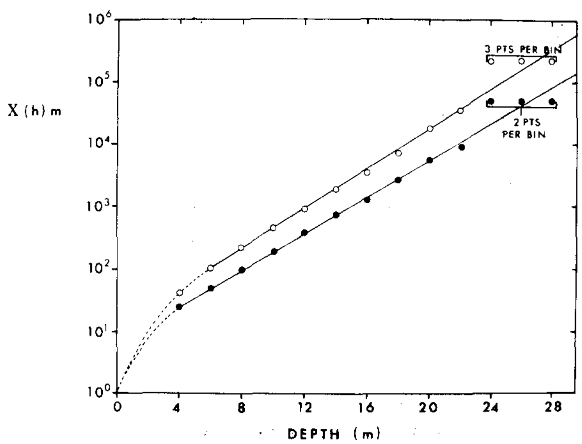

Fig. 4. $\bar{X}(h)$ plotted against h for the whole data set (open circles) and for sections 1 and 2 only (filled circles).

therefore of approximately equal efficiency. In case 1, the 1000 year return period corresponds to a depth of 53.7 m using technique 2, compared with 55.1 m for technique 1.

Technique 3: Probability plotting

A second distribution-free technique of prediction was proposed by Tucker et al. (1979) for the interpretation of laser data. The record is divided into uniform sampling intervals of convenient length; in our case a 50 km interval fits the analysis scheme used by WH. The deepest keel is extracted from each sampling interval, and the resulting keels are ranked in order of depth. The keel depths are then plotted on normal probability paper using the Weibull plotting formula

$$F = \frac{1}{P(X > x)} = \frac{n+1}{m} \tag{9}$$

where

n = total number of depth values involved (27 in our case);

m = rank of a given keel (m = 1 for the deepest keel and m = 27 for the shallowest in the set);

F = return distance in units of 50 km.

Tucker et al. found that such a plot fitted a straight line over almost the whole range of the data, with a deviation only for the highest ridges. Such a technique has also been used to predict other extreme events such as floods (Slack et al., 1975).

We have plotted the deepest keels obtained from each of the 27 sections of WH's analysis with results shown in Fig. 5 (circles). There is a good fit to a straight line for all except the four deepest keels. An

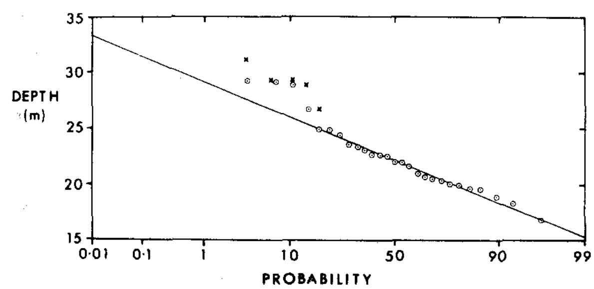

Fig. 5. Plot of recurrence probability for deepest keel in a 50 km section. Open circles use 27 sections; crosses show effect of including an additional very deep keel.

TABLE 3

Extreme depth predictions using normal probability plotting

D (m)	$P(X > x)$	F (km)	T_D, case 1
25	17.5%	285.7	3.4 months
30	0.5%	10^4	10 years
35	0.0008%	6.25×10^6	6,250 years

extrapolation of this straight line, however, produces the following predictions for return periods equivalent to case 1 for techniques 1 and 2 (Table 3). The analysis is not taken to greater depths because clearly the return periods are becoming very much larger than those predicted by the first two techniques.

The failure of this technique to fit the four deepest keels is even worse if we take account of the deepest keel in the whole record – 31.12 m – which occurred within a short stretch of track which was less than 50 km long and which was not included in WH's standard analysis. If we allow this keel to be the 28th member of the set and replot, most of the data points in Fig. 5 are shifted only a negligible distance. The four deepest keels, however, are shifted further, and their new positions, together with that of the new deepest keel, are shown as crosses in Fig. 5. The five keels now show an enhanced deviation from the extrapolated straight line, and it is clear that this technique is not valid for predicting extreme values. Even Tucker et al. found that the highest sails in their records were much higher than the predictions of probability plotting.

A somewhat similar technique is log-normal plotting, where all of the deep keels are used in the ranking (not just the deepest in each 50 km section) and the resulting depths plotted on log-normal paper

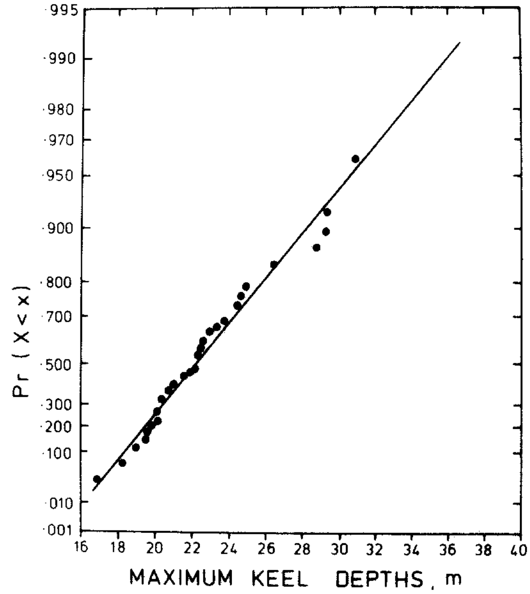

Fig. 6. Data from Fig. 5 replotted on exponential extreme-value probability paper.

rather than linear-normal as in Fig. 5. This technique also does not work for the submarine data, yielding a smooth curve instead of a straight line.

A third probability plotting method, however, shows more promise. If the same variables as in Fig. 5 are plotted on exponential extreme-value probability paper (Gumbel, 1954, 1958) the result is a much better fit to a straight line which includes the five deepest keels as well as the rest of the values (Fig. 6). This method was employed by Lewis (1977, 1978) in estimating extreme values of ice scour depth, and by Krumbein and Lieblein (1956) in studying extreme boulder diameters. Table 4 shows return periods at various depths taken from Fig. 6 and compared with techniques 1 and 2 and Fig. 5. There is good agree-

TABLE 4

Comparison of return periods, case 1

Keel depth	Technique 1	Technique 2	Technique 3 (Fig. 5)	Technique 3 (Fig. 6)
25 m	(1.6±0.05) months	(1.3±0.04) months	3.4 months	(2.6±0.2) months
30 m	(9.2±0.4) months	(8.1±0.3) months	10 years	(11.5±1.5) months
35 m	(4.3±0.2) years	(4.2±0.2) years	6250 years	(4.2±1.4) years
40 m	(24.3±1.6) years	(26.2±1.8) years		(21.5±5) years

ment between the Gumbel method and the results of techniques 1 and 2. This is to be expected if the parent distribution is a negative exponential.

Recommendations

All three of these techniques have advantages. Technique 3 (Gumbel plotting) is easiest for an analyst presented with a raw data set (e.g. a submarine profile on chart rolls) where the only analysis task required is to predict extreme depth values; he can run quickly through the data, noting only the greatest depth in each standard section length. Technique 2 has closer confidence limits while avoiding the necessity of defining a ridge arbitrarily. Technique 1 is the method that would normally be attempted first, since in most cases the analyst is interested in the entire distribution of ridge frequencies and depths as well as in predicting extremes.

EXTREME DEPTH PREDICTIONS ALONG A LINE

Basic definitions

Extreme keel depth prediction at a point has as its practical application the estimation of the return period for disturbance of a seabed installation of small dimensions, such as a wellhead. To estimate the return period for scouring by keels across a seabed pipeline route, however, requires a further dimension of analysis. Thus having determined N_D or T_D, the next step is to attempt a prediction of the number of scouring events per year along a 1 km line oriented at right angles to the mean ice drift direction. If this number, S_D say, is multiplied by the number of km of pipeline y_D that are to be constructed at this water depth (again, projected at right angles to mean ice

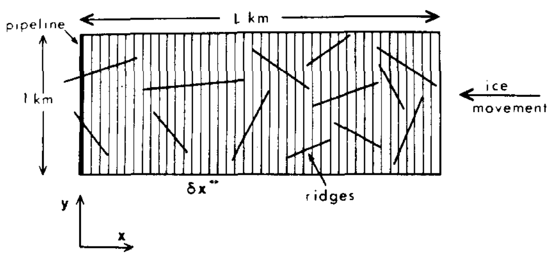

Fig. 7. The area geometry of pressure ridges.

drift direction), then we can obtain an estimate of the scouring rate along the whole pipeline as

$$\text{Scouring events per year} = \sum_D S_D y_D \tag{10}$$

The pipeline route is expressed as a sum of as many sections as are required by the varying bottom topography and varying ice conditions. We expect S_D to be linearly dependent on N_D so we can say

$$S_D = N_D f \tag{11}$$

and our problem is to calculate f.

Consider 1 km of pipeline (Fig. 7) and assume that the ice drift is always at right angles to it. The area of icefield that sweeps past the pipeline in one year is therefore L km^2. At any instant there are, on average, (N_D/L) keels intersecting the pipeline and scouring the bottom if the water depth is D, assuming that keels are statistically isotropic, i.e. randomly oriented (from eq. 5).

Now consider the "annual box" of Fig. 7 divided into narrow strips as shown of width δx. Each time that the ice moves by δx, (N_D/L) "keel linkages" are transported across the pipeline, where a "keel linkage" is defined as a section of keel, depth greater than D, and projected length δx along the x-axis. Therefore when the whole "annual box" has drifted across the pipeline, $(N_D/\delta x)$ "keel linkages" have been transported across the pipeline. Now if each keel has an average projected length l' along the x-axis, the number of *keels* that have been transported is $(N_D/\delta x)/(l'/\delta x) = (N_D/l')$. Therefore we infer

$$f = 1/l' \tag{12}$$

If keels are randomly oriented and of mean length l, then

$$l' = \frac{2l}{\pi} \int_0^{\pi/2} \cos\theta \, d\theta = 2l/\pi \tag{13}$$

so

$$f = \pi/2l \tag{14}$$

where l is the mean length of a keel in km.

This is not, unfortunately, the overall length of a keel as observable on aerial photographs. Instead, it is the length of a continuous section of keel which is deeper than D, since we have insisted in the analysis that the keels must all scour the bottom. This involves us in the problem of longitudinal keel statistics, i.e. how the depth of a keel crest varies with distance along its axis.

Estimates from keel observations

Field observations of depth variations along the crest of a keel are extremely sparse, because of the difficulty of measurement. The only available sonar profile along a keel crest was obtained by an unmanned submersible in the Beaufort Sea in 1972 and analysed in Wadhams (1976). The keel was a shallow one of mean draft 5.95 m in a floe of draft 2.58 m, so its mean relief was only 3.37 m; Wadhams published a graph of the crest coherence (1976, Fig. 21), but since the depth variations are almost certainly due to the relief of single ice blocks, the analysis is inappropriate for deeper keels. With deeper keels we expect greater absolute variations in depth along the crest, but smaller relative variations and with a tendency to a longer wavelength of variation. With normal submarine sonar profiles the angles at which ridges are crossed are not known. In fact, models of keels (e.g. Wadhams, 1978) usually assume them to be linear features of triangular cross-section, so that even an oblique crossing by submarine will generate a profile in which genuine along-crest depth variations are convolved with the flattened triangle of the keel cross-section. Valid information cannot therefore be extracted.

There are a few studies in which a keel has been cored and its dimensions examined more extensively than across a single cross-section. For instance, Wright et al. (1979) reported that three multi-year keels had lengths of 250 m, 70 m and 70 m. This suggests that we could take 100 m as an order-of-magnitude guess for l, giving an f of 16. Clearly a priority in field observations must be depth measurements along keel crests, by divers or scanning sonar.

Estimates from scour observations

In the absence of direct measurements of keel crest coherence, we can estimate l by looking at the widths of the scour marks made by the keels. l is the mean length of a keel section which is continuously deeper than D. In water of depth D, this is exactly the same as the mean width of a scour mark, provided the keel which makes the scour is oriented at right angles to the direction of scouring.

Lewis (1977) measured the mean width of scour marks as a function of water depth, along a one-dimensional sonar line running NW from Kugmallit Bay. Widths were thus projected on to a NW–SE axis, which lies approximately at right angles to the mean direction of ice drift in that vicinity. Assuming random keel orientation, then (which may not be valid in the nearshore zone), we can identify the mean projected scour width with l' in eq. (12). This gives us the values for f shown in Table 5. The values do not differ wildly from the guess made earlier. Thus we now have a means of estimating f and hence S_D in eqn. (11). The numerous sidescan sonar profiles of the Beaufort Sea shelf that are now available, both in and out of the public domain, enable estimates of f to be made in a site-specific way.

TABLE 5

Predictions of f using mean scour widths of Lewis (1977)

Water depth D (m)	l' (km)	$f = 1/l'$
15	0.0302	33.1
25	0.0313	32.0
35	0.0699	14.3
45	0.0595	16.8
55	0.0625	16.0
65	0.0628	15.9

Application to pipeline burial depths

Finally we consider a case study in which the sonar statistics are applied to the estimation of the depth required to bury a pipeline so that disturbance occurs at only a specified return period. The numbers are intended mainly for illustration, and for any real case will be subject to major revision in the light of field observations.

We assume that we wish to lay a pipeline 76 km long, the distance to shore from the Dome Petroleum "Kopanoar" well in the Canadian Beaufort Sea. We use a result discovered by Lewis (1977) and employed by Pilkington and Marcellus (1981), that the probability that a given scour mark extends to a depth d or greater below the undisturbed seabottom is exp $(-kd)$, where k is a parameter which is site-specific and which can be determined from sonar mosaics of the immediate area. Thus the number of scouring events per year per km at depth D is $S_D = N_D f$ from (11); and the return period, T, per km for a scour of depth d at water depth D is

$$T = (S_D e^{-kd})^{-1} \tag{15}$$

which gives, using negative exponential distribution of keel drafts, eqn. (5),

$$d = \frac{1}{k} \ln \left[L\mu T f \exp \left(- \frac{D - h_0}{\bar{h} - h_0} \right) \right] \tag{16}$$

d is then the required depth of burial for the top of the pipe to give a return period T of disturbance per km.

In this case, for a return period of, say, 1000 years years and a 76 km pipeline, the return period per km in (16) must be set at 76,000 years. This raises the question of what happens when further pipelines are built. If n separate pipelines of 76 km are built to the same specifications as the first, the return period for disturbance of one of them drops to $1000/n$ years. In selecting a design value for T, then, the engineer must estimate the total number of pipelines that are likely to be constructed during the life of the oilfield.

Using (16) we now calculate d at different water depths using k values from Lewis (1977), f values from Table 5, reasonable guesses for L, and ice statistics from section 1 of the "Gurnard" profile (h_0 = 9 m $\bar{h}$ = 12.15 m, μ = 5.11 km^{-1}). The results are shown in Table 6.

The required trench depths at 1000 yr return period lie in the range 6.2 to 9.6 m, which is well beyond the capacity of currently available trenching methods. It is significant that the required trench depth is high even at the extreme water depth of 65 m where the scouring frequency is very low. This is because those scours which do occur tend to be very deep ones, hence the low k value. The low k then compensates for the high D in (16). This prediction should be revised downwards if some of the scours at great water depths, contributing to the low k, could be shown to be relict, as interpreted by Lewis (1977, 1978).

In any real application the parameters used in (16) must be determined by site-specific measurements. This applies to the keel depth distribution as well as the scour depth distribution, since local variations in bottom topogtaphy may prevent floes which contain deep keels from approaching the experimental site. The most difficult problem, and one for which a solution has not yet been devised, is to obtain a k-value for recent scours only, which may be significantly different from the k for all scours. Otherwise, there is no evidence at present that any of the assumptions used to derive (16) are invalid. One might expect *a priori* that an absolute upper limit exists for scouring depth due to the mechanical properties of the sediment, just as one might postulate an absolute upper limit for pressure ridge keel depth. However, data analysed so far have not revealed such an upper limit: in a recent analysis by Weeks et al. (1983) of the extensive Alaskan scour data no deviation from a negative exponential was found over four decades of scour frequency, while analyses of long sonar profiles have also shown no anomalous scarcity of very deep keels (e.g. Wadhams, 1978). Until evidence of upper limits is found, a conservative assumption must be that observed distributions of keel depth and of scouring depth can be extrapolated to predict extremes.

TABLE 6

Trench depths to top of pipeline for 1000, 100 and 10 year return periods

Water depth D (m)	k	f	L	Trench depth d (m)		
				1000 yr	100 yr	10 yr
15	3.120	33.1	150	6.24	5.50	4.76
25	2.129	32.0	400	8.10	7.02	5.94
35	1.775	14.3	600	7.70	6.40	5.11
45	1.142	16.8	800	9.59	7.57	5.56
55	1.148	16.0	1000	6.92	4.91	2.91
65	0.725	15.9	1200	6.83	3.65	0.48

ACKNOWLEDGEMENTS

I am indebted for useful discussions to Roger Pilkington (Dome Petroleum Ltd., Calgary), Bob Marcellus (Canada Marine Engineering, Calgary), Donald Gaver and Pat Jacobs (U.S. Naval Postgraduate School, Monterey) and Mike Lewis (Geological Survey of Canada, Dartmouth). I thank Rob Massom for diagrams and Ruth Weintraub for computing. I am grateful to the Office of Naval Research for support under Contract N00014-80-G-0002, and to the Arctic Submarine Laboratory, San Diego, for the original release of submarine data.

REFERENCES

Gumbel, E.J. (1954).. Statistical theory of extreme values and some practical applications. U.S. Natl. Bureau of Standards, Applied Maths. Series, 33, 51 pp.

Gumbel, E.J. (1958). Statistics of Extremes. Columbia Univ. Press, New York, 375 pp.

Hibler, W.D. III, W.F. Weeks and S.J. Mock (1972). Statistical aspects of sea-ice ridge distributions. J. Geophys. Res., 77(30): 5954–5970.

Hoare, R.D., B.W. Danielewicz, G.R. Pilkington, J.C. O'Rourke and R.D, Wards (1980). An upward-looking sonar system to profile ice keels for one year. Oceans '80, Conf. on Ocean Engng. in the '80's, Seattle, 8–10 Sept. 1980. Inst. Electrical & Electronic Engrs., New York, pp. 123–126.

Krumbein, W.C. and J. Lieblein (1956). Geological application of extreme-value methods to interpretation of cobbles and boulders in gravel deposit. Trans. Amer. Geophys. U., 37(3): 313–319.

Leppäranta, M. (1981). Statistical features of sea ice ridging in the Gulf of Bothnia. Winter Navigation Res. Bd., Helsinki, Tech. Rept. 32.

Lewis, C.F.M. (1977). Bottom scour by sea ice in the southern Beaufort Sea. Dept of Fisheries & Envt., Ottawa; Beaufort Sea Project Tech. Rept. 23.

Lewis, C.F.M. (1978). The frequency and magnitude of drift ice groundings from ice scour tracks in the Canadian Beaufort Sea. In: D.B. Muggeridge (Ed.), Proc. 4th Intl. Conf. on Port & Ocean Engng. Under Arctic Condns. Memorial Univ., St. John's, Vol. 1, pp. 568, 579.

Lowry, R.T. and P. Wadhams (1979). On the statistical distribution of pressure ridges in sea ice. J. Geophys. Res., 84: 2487–2494.

NORCOR (1977). Probable behaviour and fate of a winter oil spill in the Beaufort Sea. Rept. EPS 4-EC-77-5 by NORCOR Engng. & Res. Ltd., Yellowknife, to Envtl. Protection Service, Dept. of Fisheries & Envt., Ottawa.

Pilkington, G.R. and R.W. Marcellus (1981). Methods of determining pipeline trench depths in the Canadian Beaufort Sea. Proc. 6th Intl. Conf. on Port & Ocean Engng. under Arctic Conditions. Quebec, Aug. 1981, Vol. 2, pp. 674–687.

Slack, J.R., J.R. Wallis and N.C. Matalas (1975). On the value of information to flood frequency analysis. Water Resources Res., 11: 629–647.

Thorndike, A.S. and R. Colony (1980a). Large-scale ice motion in the Beaufort Sea during AIDJEX, April 1975–April 1976. In: R.S. Pritchard (Ed.), Sea Ice Processes and Models. Univ. Washington Press, Seattle, pp. 249–260.

Thorndike, A.S. and R. Colony (1980b). Arctic Ocean Buoy Program. Data report, 19 January 1979–31 December 1979. Polar Science Center, Univ. Washington.

Thorndike, A.S. and R. Colony (1981). Arctic Ocean Buoy Program. Data report, 1 January 1980–31 December 1980. Polar Science Center, Univ. Washington.

Tucker, W.B., III, W.F. Weeks and M. Frank (1979). Sea ice ridging over the Alaskan continental shelf. J. Geophys. Res., 84: 4885–4897.

Wadhams, P. (1976). Sea ice topography in the Beaufort Sea and its effect on oil containment. AIDJEX Bull., 33: 1–52.

Wadhams, P. (1978). Characteristics of deep pressure ridges in the Arctic Ocean. In: D.B. Muggeridge (Ed.), Proc. 4th Intl. Conf. on Port & Ocean Engng. Under Arctic Conditions, Memorial Univ., St. John's, Vol. 1, pp. 544–555.

Wadhams, P. (1980). A comparison of sonar and laser profiles along corresponding tracks in the Arctic Ocean. In: R.S. Pritchard (Ed.), Sea Ice Processes and Models. Univ. Washington Press, Seattle, pp. 283–299.

Wadhams, P. (1981) Sea-ice topography of the Arctic Ocean in the region 70°W to 25°E. Phil Trans. Roy. Soc., London, A302 (1464): 45–85.

Wadhams, P. and R.J. Horne (1980). An analysis of ice profiles obtained by submarine sonar in the Beaufort Sea. J. Glaciol., 25 (93): 401–424.

Wadhams, P. and R.T. Lowry (1977). A joint topside-bottomside remote sensing experiment on Arctic sea ice. Proc. 4th Can. Symp. Remote Sensing, Quebec, May 1977. Can. Remote Sensing Soc., Ottawa, pp. 407–423.

Weeks, W.F., W.B. Tucker, III, M. Frank and S. Fungcharoen (1980). Characterization of the surface roughness and floe geometry of the sea ice over the continental shelves of the Beaufort and Chukchi Seas. In: R.S. Pritchard (Ed.), Sea Ice Processes and Models. Univ. Washington Press, Seattle, pp. 300–312.

Weeks, W.F., P.W. Barnes, D.M. Rearic and E. Reimnitz (1983). Statistical aspects of ice gouging on the Alaskan Shelf of the Beaufort Sea. In: P. Barnes, D. Schell and E. Reimnitz (Eds.), The Beaufort Sea – Physical and Biological Environment. In press.

Williams, E., C.W.M. Swithinbank and G. de Q. Robin (1975) A submarine sonar study of Arctic pack ice. J. Glaciol., 15: 349–362.

Wright, B., J. Hnatiuk and A. Kovacs (1979). Multi year pressure ridges in the Canadian Beaufort Sea. Proc. 5th Intl. Conf. on Port & Ocean Engng. Under Arctic Condns., Univ. Trondheim, Vol. 1, pp. 107–126.